Numerical Study of the Harmonic Oscillator Using RK4

Tomasz Karpiński

October 21, 2025

Abstract

This short report presents a numerical study of the one-dimensional harmonic oscillator and its damped and driven variants. The ordinary differential equation of motion is integrated using the classical fourth-order Runge–Kutta (RK4) method. Results include time-domain trajectories, phase-space portraits and energy evolution and the driven steady-state amplitude versus driving frequency. Figures and a compact discussion accompany the numerical results.

1 Introduction

The one-dimensional harmonic oscillator is a fundamental model in classical mechanics. Its equation of motion can be written as

$$m\ddot{x} + \alpha\dot{x} + kx = F_0 \sin(\omega_{\text{ext}} t), \tag{1}$$

where m is the mass, k the spring constant, α a friction parameter and $F_0, , \omega_{\text{ext}}$ the amplitude and angular frequency of an external driving force. This report focuses on: (i) the conservative oscillator ($\alpha = 0, , F_0 = 0$), (ii) the damped free oscillator ($\alpha > 0, , F_0 = 0$), (iii) the effect of varying damping, and (iv) the driven steady-state response as a function of driving frequency.

2 Numerical method

Equation (1) is rewritten as a first-order system by introducing the velocity $v = \dot{x}$ and the state vector

$$u = \begin{pmatrix} x \\ v \end{pmatrix}, \qquad u' = f(u, t)$$

Integration is performed with the classical fourth-order Runge–Kutta method (RK4) with fixed time step Δt. For a general nonautonomous system $u' = f(u, t)$ the RK4 update from t_n to $t_{n+1} = t_n + \Delta t$ is

$$\begin{aligned} k_1 &= f(u_n, t_n), \\ k_2 &= f\Big(u_n + \tfrac{\Delta t}{2} k_1, \; t_n + \tfrac{\Delta t}{2}\Big), \\ k_3 &= f\Big(u_n + \tfrac{\Delta t}{2} k_2, \; t_n + \tfrac{\Delta t}{2}\Big), \\ k_4 &= f\Big(u_n + \Delta t \, k_3, \; t_n + \Delta t\Big), \\ u_{n+1} &= u_n + \frac{\Delta t}{6}\big(k_1 + 2k_2 + 2k_3 + k_4\big). \end{aligned}$$

Applied to the two-component state $u = (x, v)^T$, the stage vectors have two components; writing $k_i = (k_{i,x}, k_{i,v})^T$ we obtain, for example,

$$x_{n+1} = x_n + \frac{\Delta t}{6}\big(k_{1,x} + 2k_{2,x} + 2k_{3,x} + k_{4,x}\big), \qquad v_{n+1} = v_n + \frac{\Delta t}{6}\big(k_{1,v} + 2k_{2,v} + 2k_{3,v} + k_{4,v}\big),$$

with

$$k_{i,x} = v^{(i)}, \qquad k_{i,v} = -\frac{k}{m}x^{(i)} - \frac{\alpha}{m}v^{(i)} + \frac{F_0}{m}\sin(\omega_{\text{ext}}t^{(i)}),$$

where $(x^{(i)}, v^{(i)})$ and $t^{(i)}$ denote the stage input state and time for the i-th stage.

Energy diagnostics were computed each time step as

$$E_{\text{kin}} = \tfrac{1}{2}mv^2,$$
$$E_{\text{pot}} = \tfrac{1}{2}kx^2,$$
$$E_{\text{tot}} = E_{\text{kin}} + E_{\text{pot}}.$$

The RK4 scheme is explicit and fourth-order accurate in time. Time-step Δt and total integration time were chosen to ensure that transients decay for driven simulations and that the numerical error remains small compared to the physical effects we investigate.

3 Results

3.1 Conservative oscillator

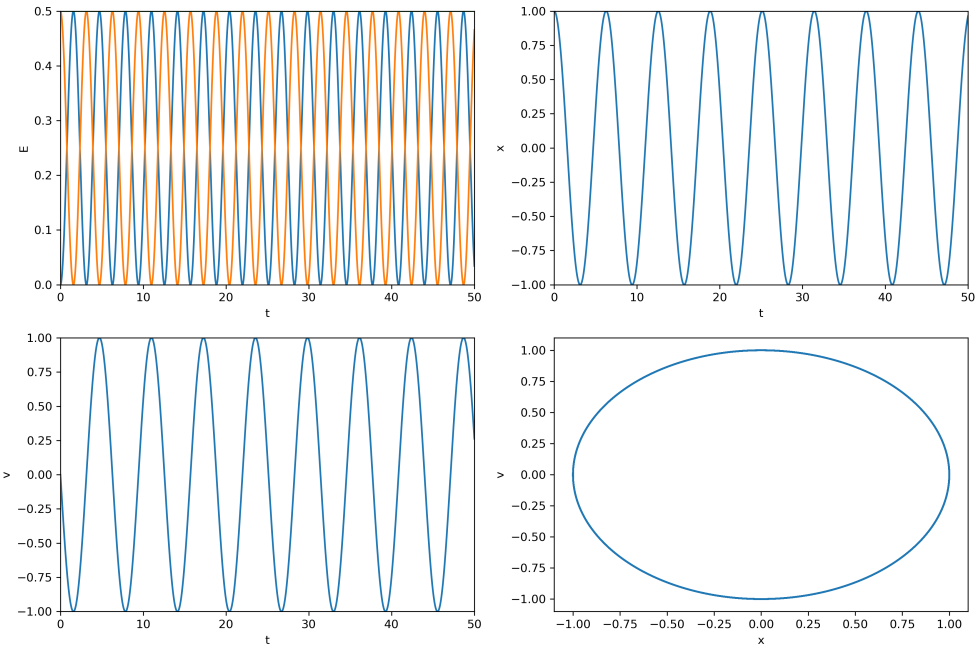

Figure 1: Undamped, undriven oscillator. The plots show (from top-left, clockwise): Energy vs. Time, Displacement $x(t)$, Phase-space $v(x)$, and Velocity $v(t)$.

The Top-Right and Bottom-Left plots show sustained, non-decaying sinusoidal waves for displacement and velocity respectively. The Top-Left plot shows kinetic and potential energy oscillating perfectly out of phase while the total energy remains constant, confirming energy conservation. The Bottom-Right phase-space plot is a closed ellipse, characteristic of a conservative periodic system.

3.2 Damped oscillator

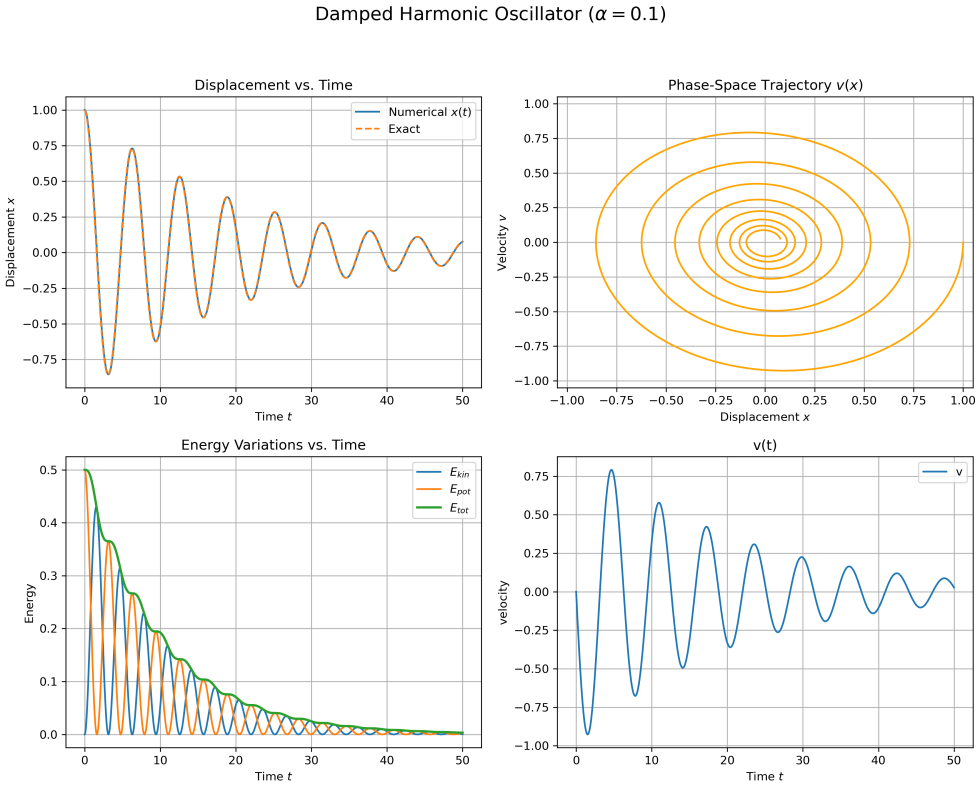

Figure 2: Damped free oscillator (example $\alpha = 0.1$). The plots show (from top-left, clockwise): Displacement $x(t)$ (Numerical vs Exact), Phase-space $v(x)$, Velocity $v(t)$, and Energy variations.

The top-left plot compares the numerical solution $x(t)$ with the exact analytical formula for the underdamped case; the two curves are in very good agreement. The phase-space figure demonstrates a spiraling trajectory toward the origin, showing energy loss. The energy plot displays kinetic and potential components exchanging while total energy decays monotonically. The velocity plot complements the displacement view and highlights the damping of the motion.

3.3 Sweep of damping coefficients

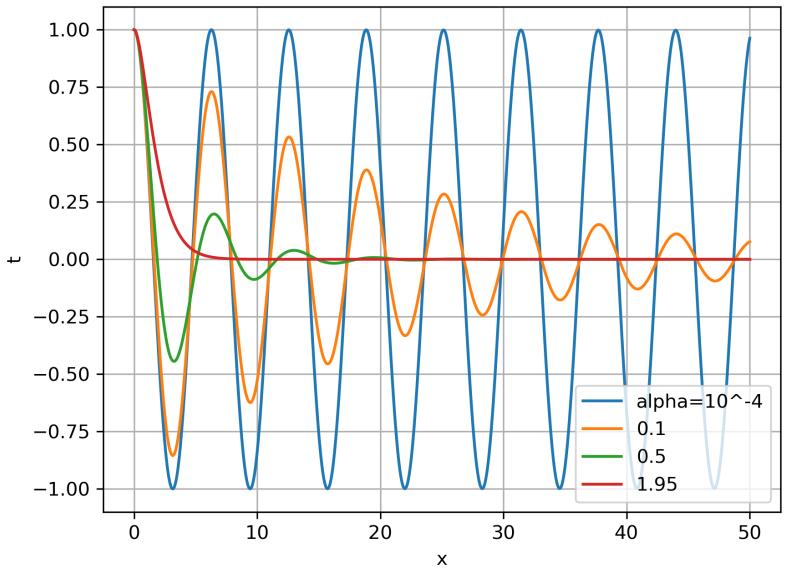

Figure 3: Comparison of time-series / amplitudes for several α values.

The figure compares behavior for multiple damping parameters. Larger α results in faster decay of oscillation amplitude and a quicker approach to equilibrium. Small damping keeps the oscillations visible for many cycles; the figure succinctly demonstrates the continuous transition from almost-conservative to heavily-damped regimes.

3.4 Driven steady-state amplitude

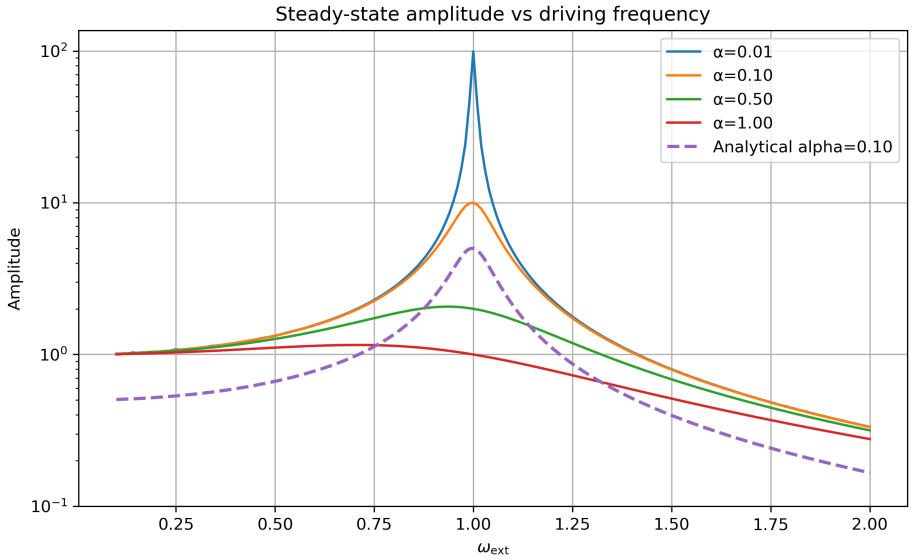

Figure 4: Steady-state amplitude $x_{\max}(\omega_{\text{ext}})$ for several α (log–log scale for clarity).

The resonance curves display a peak near the system natural frequency; the peak is sharper and higher for smaller damping. The log–log presentation emphasises the scaling of the response over several decades and makes it easier to compare the tails at low and high driving frequency.

4 Conclusions

This project implemented a robust and easily reusable RK4 integrator to study the harmonic oscillator in conservative, dissipative and driven regimes. Numerical results reproduce known analytical behavior: energy conservation in the undamped case, exponential decay of amplitude and energy in the damped case, and a resonance peak for the driven system whose height and width depend on the damping coefficient. Comparing numerical and analytical solutions in the underdamped case shows excellent agreement, validating both the implementation and parameter choices (time-step and total integration time) used here.

The sweep across damping values clearly illustrates that larger friction accelerates the disappearance of transient oscillations and reduces the steady-state response; quantitatively, the amplitude decays roughly exponentially with a rate proportional to $\alpha/(2m)$ in the small-damping limit. The last part shows steady-state amplitude: as α grows the resonance peak diminishes and broadens, and the numerical maxima align well with the analytical prediction for the linear forced oscillator.

Overall, the RK4 method provided a reliable compromise between accuracy and computational cost for the time spans considered.